Passive Seismic Monitoring of Reservoirs: A Case Study from Oman

A. Al-Anboori[1, 3] and J-M. Kendall[2]

Introduction

The passive monitoring of microseismic events can provide an inexpensive and effective means of monitoring spatial and temporal variations in reservoir properties. Those microearthquakes will occur naturally because of tectonic stresses but also can be induced through exploitation activities such as hydraulic stimulation, enhanced petroleum recovery, and fluid extraction. Such monitoring offers insights into the dynamic state of stress in a reservoir — invaluable information for developing effective strategies for drilling, injection, and production programs.

Although microseismic monitoring has been used to study geothermal fields since the 1970s, the oil industry started to realize its potential only recently. Microseismic monitoring was relatively uncommon in oil fields 10 years ago, but it is now fairly commonplace in monitoring the hydraulic stimulation of fractures, for example. The processing of such data is quite different from approaches used in conventional reflection seismology. In fact, the techniques used are more akin to those used in conventional earthquake seismology.

The use of microseismic data can be divided into two broad categories: (1) the study of the source itself and (2) imaging of the surrounding medium. Sudden stress release on faults and fractures will generate elastic waves that will propagate into the surrounding medium. The first step in any microseismicity study is to locate those events as accurately as possible. Their locations and how they migrate in time can be used to image fault planes, to infer fault reactivation, and to monitor the propagation of perturbations to the stress field. That can be important in detecting compartmentalization in reservoirs, assessing caprock integrity, and monitoring injection fronts. Directional variations in the pattern of energy release at the source can be used to determine the orientation and magnitude of the stress field and to further assess the orientation and motion of fault planes.

Given sufficient source-and-receiver coverage, microseismic data can be processed by using imaging tools such as tomography and velocity analysis. Because both P-wave and S-wave signals are generated and recorded, much potential exists to determine lithologic and fluid properties from P- and S-wave velocities and their ratios. Furthermore, such data are suited ideally to the study of seismic anisotropy. Unlike conventional reflection seismology, raypaths are not generally vertical, and hence, directional variations in velocity are assessed more easily. Perhaps the most unambiguous indicator of anisotropy is shear-wave splitting. Measurements of such splitting can be used to assess fracture properties, which are sensitive to spatial and temporal variations in the stress field. Finally, microseismic data are generally rich in frequency content, and much potential exists to evaluate frequency-dependent wave phenomena. For example, they can be used to estimate effective Q. It also has been shown that frequency-dependent shear-wave splitting is sensitive to crack size, aspect ratio, and fluid properties.

In this paper, we illustrate some of the potential uses of microseismic data in reservoir decision making through a case study of a data set acquired in a large oil field in west-central Oman. The intent is to illustrate the broad range of applications of passive seismic monitoring and to highlight the rich potential that such data sets have in reservoir management.

The Oman data set

A recent passive seismic experiment in Oman provides one of the best monitoring arrays so far. Data were

[1]University of Leeds, School of Earth and Environment, Leeds, U. K.
[2]University of Bristol, Department of Earth Sciences, Bristol, U. K.
[3]Petroleum Development Oman, Study Center, Oman.

acquired by recording tools deployed in five boreholes at depths between 800 m and 1400 m (Figure 1). The wells lie proximal to two large graben faults that trend northeast-southwest through the center of the field. The sensor array in each well is comprised of eight four-component receivers (tetrahedral configuration; see Jones and Asanuma [2004]). In this paper, we present results from the analysis of 15 days of data, during which time 641 locatable events were identified, with an average of nearly 43 events per day. An additional 26 large events that were recorded during a seven-day period supplement the data set.

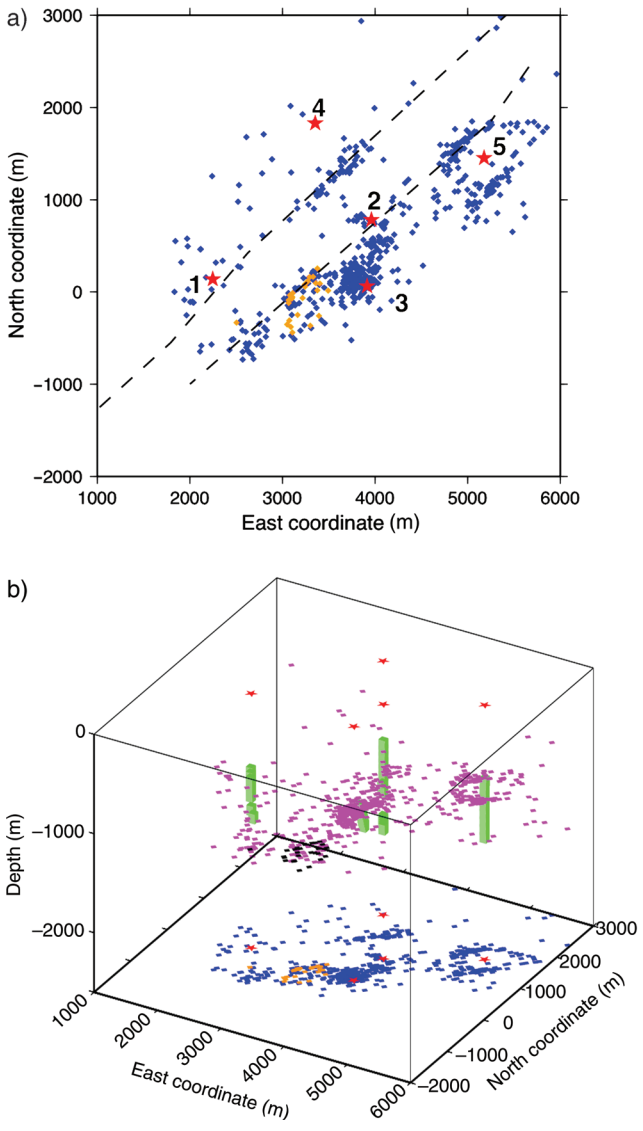

Figure 1. Event locations for the Oman data set. Red stars mark surface location of the recording boreholes. (a) Dashed lines that trend northeast-southwest mark large graben faults that transect the field. Blue symbols mark located events from a two-week period, and orange symbols mark large events from another week of data. (b) Green cubes show sensor locations in each of the five boreholes, pink and black symbols show the event locations in three dimensions, and blue and orange symbols show the locations projected onto the base of the map.

The monitoring covers a region of two carbonate reservoirs: an upper gas reservoir (the Natih A Formation) and a lower oil reservoir (the Shuaiba Formation). The Fiqa and Nahr Umr shale formations act as caprocks to the upper and lower reservoirs, respectively. The field is domelike in shape because of deep-seated salt movement. Major faults in the field trend southeast-northwest or northeast-southwest. The latter are high-angle normal faults, a result of the extensional regime associated with salt uplift and forming a northeast-trending graben system. The faults that trend southeast-northwest show strike-slip movement and are associated with later-stage regional tectonics because of the collision of the Arabian and Eurasian Plates.

Source locations

The quality of any study that uses microseismic data is limited by the accuracy of event locations. That accuracy is controlled directly by the number and spatial distribution of receivers, accuracy of the velocity model, quality of traveltime picks and, if necessary, accuracy in estimates of particle-motion directions.

Until recently, most oil-field microseismic data sets were acquired by using sensors deployed in a single borehole. Part of the reason for using a single borehole was that sensor deployment required the drilling of a monitoring well or that the experiment resulted in one less production borehole, with both options being costly. However, recent advancements in borehole technology have led to the design of tools that can be deployed in producing wells (see Wilson et al., 2004). The receiver effectively is coupled to the surrounding rock while being decoupled from flowing material in the well. More recently, high-quality data sets have been acquired in experiments in which receivers have been deployed in multiple wells (Jones et al., 2004).

For a given velocity model, the delay time between P- and S-waves can be used to estimate the distance to the source. For a single receiver in a homogeneous medium, that distance estimate will place the source location anywhere on a sphere centered on the receiver. Recording the same event at three or more receivers deployed in different locations will constrain the location of the event. However, if the receivers all lie in a single well, the source might lie anywhere on a circle around the borehole. Locating seismic events by using sensor arrays deployed in a single borehole therefore also requires measurements of particle motions to determine what

direction the seismic energy arrives from. To invert those data for source locations, one needs to calculate traveltimes and particle-motion directions at each receiver, which can be challenging in 3D models. Unfortunately, there still will be a 180° ambiguity as to what side of the borehole the event lies on.

The Oman data set is one of the few in which multiple wells have been used. Hence, source locations are more accurate and — perhaps more important — errors in source location are more realistic than those obtained from single-well data. The region has a high level of production-related seismicity. Figure 1 shows the events analyzed in this work. Two large border faults run through the field and the events cluster near those features, but less seismicity exists in the region between faults than on the other sides of faults.

Other studies have shown that on closer inspection, seismicity clusters on a subset of preexisting faults and is most abundant in the shallow Fiqa Shale (Jones et al., 2004; Bourne et al., 2006). Jones et al. (2004) also report successful monitoring of water movement from a deep injector well. Furthermore, the locations have helped to delineate areas of reservoir compartmentalization, the edges of which pose a potential drilling hazard (Jones et al., 2004). Those findings demonstrate the links between microseismic activity and reservoir-production processes.

Focal mechanisms and stress tensor estimation

In addition to obtaining better source locations, an advantage of recording microseismic data in multiple boreholes is that the data can be used to study source mechanisms. That is not possible with receivers deployed in close proximity to one another in a single borehole; it generally requires receivers in more than one well. Fault-plane solutions or images of focal mechanisms reveal the orientation of the fault and its sense of failure. Furthermore, multiple fault mechanisms can be inverted for principal stress directions (e.g., Gephart and Forsyth, 1984). Those are standard procedures in more conventional earthquake analysis.

Few previous studies have had the geometry and data coverage to study source mechanics. Fault-plane solutions and moment tensors have been analyzed by using a data set acquired during hydraulic fracturing in the Carthage gas field in east Texas (Eisner and Sileny, 2004; Rutledge et al., 2004). Events from an interbedded sand-and-shale sequence in the Cotton Valley Formation show strike-slip faulting along vertical fracture trends confined to the more competent sandstones. This paper shows how such analyses of source mechanisms provide insights into style of faulting and fluid flow caused by injection.

We have determined 43 reliable fault-plane solutions for the Oman field. Al-Anboori et al. (2006a) summarize the methodology used in determining fault-plane solutions. We use the polarity of P- and S-wave arrivals and the relative amplitudes of the P, SH, and SV signals to determine the fault-plane solutions by using the methodology outlined in Snoke et al. (1984).

A key control step in the analysis is the use of reflectivity modeling to assess the reliability of the solutions. Determining fault-plane solutions with downhole data is considerably more challenging than with more conventional surface recordings. The signals can arrive from above or below a receiver, and with structurally complex sedimentary structures, considerable complications can be associated with ray multipathing and head-wave arrivals. The synthetics for the Oman data set show that fault-plane solutions can be retrieved uniquely by using signal polarities and amplitude ratios with receivers in as few as three wells. It is difficult to determine fault-plane solutions confidently for distant events because of contamination from first-arriving head waves.

A transition in the style of faulting appears to correlate with lithology and proximity to the major graben faults in the field. Shear movements near the easternmost graben fault show depth-dependent faulting mechanisms (Figure 2) — a transition from oblique thrust faulting with a strike-slip component in the Fiqa caprock to pure thrust faulting in the gas-charged Natih A reservoir and a transition from strike-slip faulting in the Nahr Umr caprock to more normal faulting in the oil-bearing Shuaiba reservoir. Given the normal graben faults and the extensional regime that the field is experiencing (Litsey et al. 1986), the normal faulting regime in the Shuaiba reservoir is perhaps

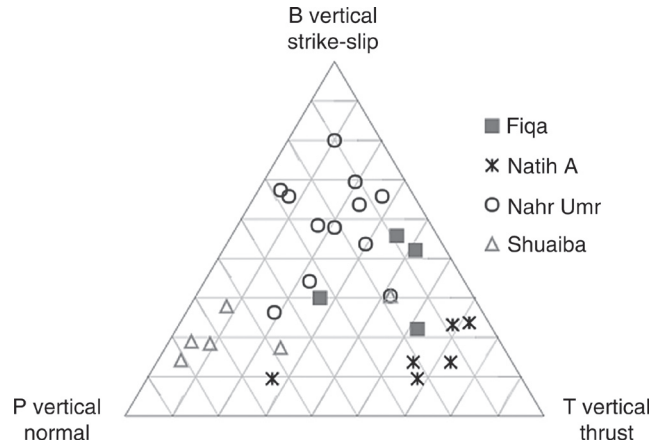

Figure 2. Summary of fault-plane solutions shows variations in source mechanisms for events confined to the Fiqa, upper Natih, Nahr Umr, and Shuaiba Formations.

not unexpected. The observed thrusting in the Fiqa caprock (with a significant strike-slip component) and in the Natih A reservoir is believed to be related to subsidence and deformation because reverse fault mechanisms are expected above compacting zones (Segall, 1989). The highest potential for compaction is the chalky Natih zone, where soft and heterogeneous units are present and pressure is reduced because of gas depletion. In addition, the faulting regime appears to be related to lithology because both shale caprocks (Fiqa and Nahr Umr) show significant strike-slip components.

The fault-plane solutions also can be used to predict the stress field in the four horizons, assuming that maximum, intermediate, and minimum stress orientations are parallel to the P- (pressure), B- (null), and T- (tension) axes, respectively. Al-Anboori et al. (2006a) show that the P-axis is predominantly horizontal in Fiqa and Natih A, subhorizontal in Nahr Umr, and subvertical in Shuaiba. The maximum stress direction therefore is predicted to be subhorizontal in the Fiqa, Natih A, and Nahr Umr and subvertical in the Shuaiba. However, the subhorizontal P-axis in Fiqa, Natih A, and Nahr Umr varies greatly in azimuth, rendering estimation of maximum stress azimuth difficult.

In Natih A, Nahr Umr, and Shuaiba, subvertical stress is more constrained and is predicted to represent minimum, intermediate, and maximum stress, respectively. That might imply that vertical stress increases with depth, as would be expected if pore pressure remains hydrostatic. That also might suggest that the vertical stress is below the maximum and minimum horizontal stress (σ_H, σ_h) in the Fiqa and Natih A, that it increases above σ_h but remains below σ_H in Nahr Umr, and finally that it exceeds both horizontal stresses σ_H, σ_h in Shuaiba.

Although source locations can delineate fault reactivation and directions of rupture, analysis of fault-plane solutions reveals the sense of motion on the fault, orientation of the stress field, and variations in fault mechanics with lithology. That is important information for several reservoir-management decisions, including assessing wellbore stability and predicting sites of potential shear failure of casing, and it might prove useful for groundtruthing geomechanical models.

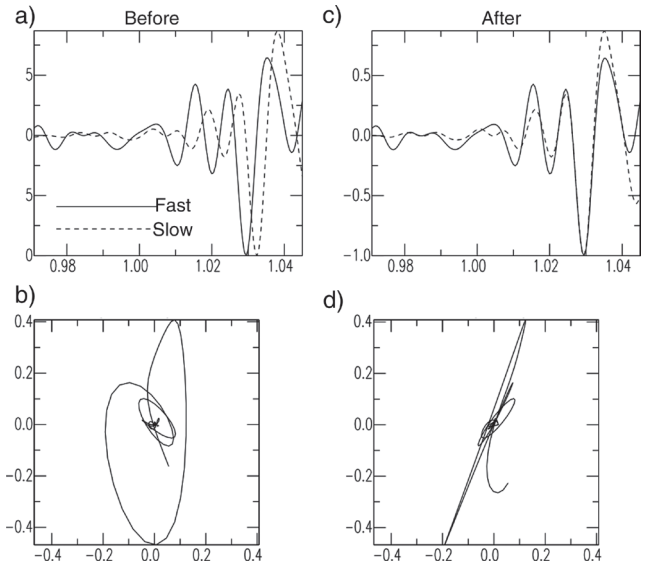

Figure 3. Example of a correction for shear-wave splitting. (a) Isolated fast and slow shear waves. (b) Particle motion, which is elliptical because of the time lag between fast and slow shear waves. (c) Fast and slow shear waves with the time lag removed, resulting in (d) linearized particle motion. In practice, the splitting parameters are determined by a grid search over delay time and fast shear-wave polarization (see Teanby et al., 2004b).

Studies of shear-wave splitting

Studies of anisotropy are useful because they provide insights into lithologic fabric and the alignment of grain boundaries, pores, cracks, and fractures. For example, anisotropy resulting from mica alignment will be sensitive to variations in compaction in shales, which can be useful in assessing shale-gas and caprock sealing properties. The preferred orientation of cracks, fractures, and joint sets also will lead to anisotropy. P-waves propagate faster parallel to fractures than in crosscutting directions and hence are sensitive to permeability anisotropy. In general, anisotropy results from a superposition of various effects. Indeed, one of the difficulties in its interpretation is discrimination among competing mechanisms (Kendall et al., 2007).

Perhaps the easiest way of detecting anisotropy by using microseismic data is through evidence of shear-wave splitting (Figure 3). Two orthogonally polarized and independently traveling shear waves will propagate in anisotropic media. The delay time (δt) between the fast and slow shear waves is proportional to the magnitude and extent of the anisotropy. Polarizations of the fast (ϕ) and slow shear waves are indicators of the anisotropic symmetry of the medium. Measurements of those two splitting parameters (δt and ϕ), coupled with observations for a range of propagation directions, can be used to characterize the anisotropy. One of the advantages of using microseismic data to study anisotropy is that the sources often are well distributed around receivers.

Evidence of shear-wave splitting in microseismic data sets has been used to infer spatial and temporal variations in fracture properties and hence variations in the stress field. For example, Teanby et al. (2004a) find evidence for that in a data set from the Valhall field in the Norwegian sector of the North Sea. They interpret the

shear-wave splitting as having been caused by an orthorhombic anisotropy resulting from superposition of vertical fractures on a mud rock with a simple transversely isotropic symmetry. They observe temporal variations in the magnitude of the shear-wave splitting during the two-month period of the experiment (Figure 4). Despite that provocative result, the experiment was too short in duration to determine whether temporal variations were caused by production and/or tidal effects. Careful comparison with production data and geomechanical reservoir models is needed to understand such effects better.

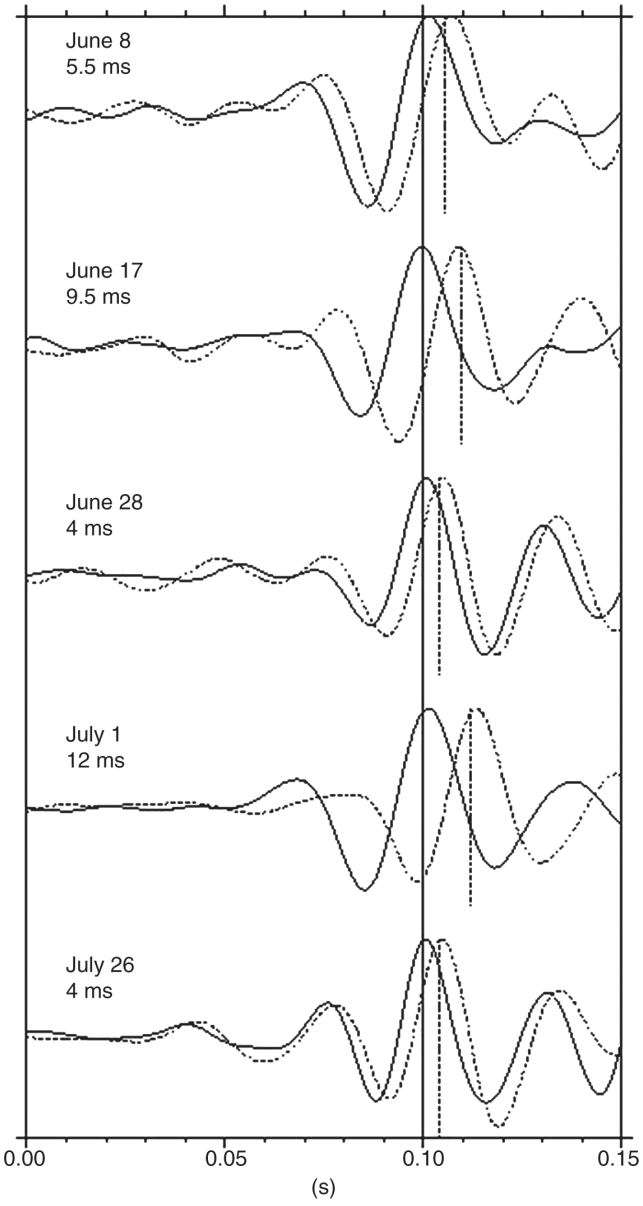

Figure 4. Example of temporal variations in shear-wave splitting for effectively colocated events. The data, which are from the 1997 Valhall experiment, show a pronounced variation in delay time between fast and slow shear waves. From Teanby et al., 2004a.

The Oman data set has yielded nearly 2500 measurements of shear-wave splitting, but only 400 of them produced reliable results. The highest values of anisotropy (as much as 10%) occur in the fractured upper parts of the carbonate gas reservoir, whereas the smallest values (~1%) occur in the lower, nonproducing, unfractured parts of the same formation (Figure 5). The Fiqa Formation shows moderate amounts of anisotropy (3–5%). Interestingly, the anisotropy also seems to be controlled by proximity to the large border faults, the largest magnitudes lying southeast of the easternmost graben fault and the lowest lying in the region between the two faults.

Care must be taken in interpreting the results of shear-wave splitting from such data. Figure 6 illustrates the

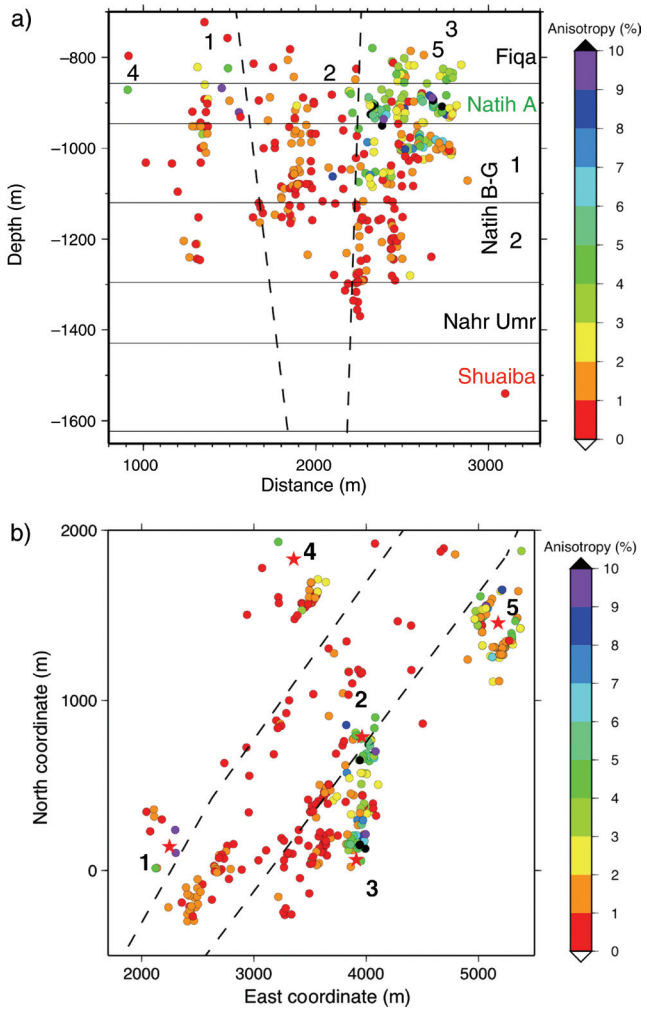

Figure 5. (a) Cross section and (b) map view of variations in anisotropy throughout the Oman field. Circles show the average anisotropy along the raypath and are plotted at the midpoint between the source and receiver. The depth section is oriented northwest-southeast, crosscutting the graben faults. Green and blue symbols mark regions of strong anisotropy; orange and red mark regions of weak anisotropy.

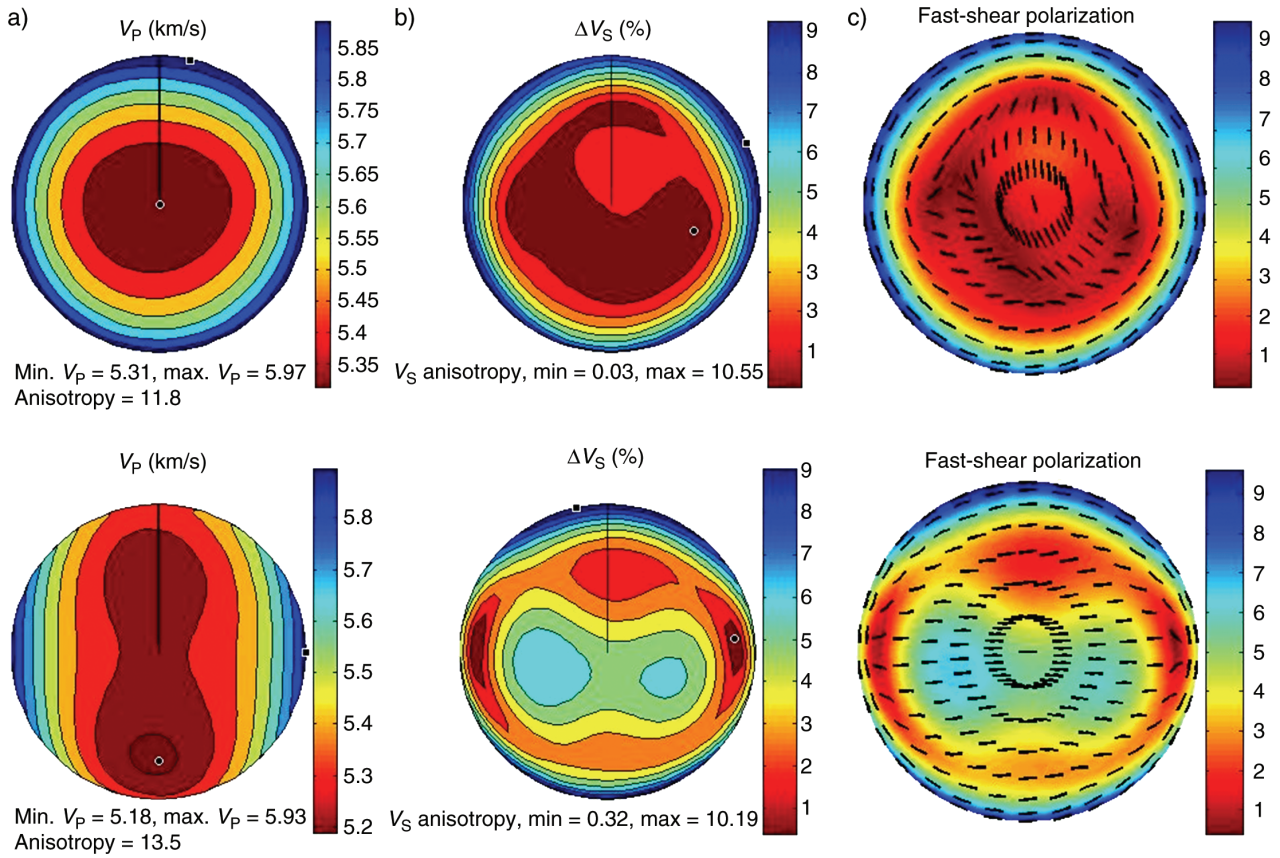

Figure 6. Variations in P-wave velocities and shear-wave splitting plotted on upper-hemisphere projections. The center of the hemisphere corresponds to vertical wave propagation, whereas the perimeter of the hemisphere shows azimuthal variations in horizontal velocities (normally those in the bedding plane). (a) Maximum and minimum P-wave velocity and P-wave anisotropy $100 \times (V_{max} - V_{min})/V_{ave}$ also are given below each hemisphere. (b) and (c) show variations in shear-wave splitting on a lower-hemisphere projection. Shear-wave splitting is expressed as a percent and is defined as $100 \times (Vs_{fast} - Vs_{slow})/Vs_{ave}$ for a given direction of wave propagation. (b) Maximum and minimum splitting are given below the hemispheres. (c) Ticks on the hemispheres show polarizations of the leading (fast) shear wave for a given direction of wave propagation. The top row shows results for rock where anisotropy is controlled by microcrystal alignment (see details in Kendall et al., 2007). The bottom row shows anisotropy in the same rock, but vertically aligned cracks, oriented left to right across the page, are superimposed on the intrinsic crystal anisotropy. The cracks do not significantly change the magnitude of the anisotropy, only the symmetry of the anisotropy. The uncracked sample has a nearly vertical transverse isotropy symmetry, whereas the cracked sample has a nearly orthorhombic symmetry.

trade-off between fracture-induced anisotropy and more intrinsic anisotropy caused by alignment (see discussion in Kendall et al., 2007). As fracture-induced anisotropy starts to dominate, subhorizontally propagating shear waves will be very sensitive to the dip of a fracture set but not to the strike. The opposite is true for waves that travel nearly vertically. Al-Anboori et al. (2005) discuss that in detail.

The average fracture dip is 73° for the Oman data set. The dominant strike of the fast shear wave is approximately 15°, but there is a secondary orientation of approximately 84° (Figure 7). The north-northeast–south-southwest orientation agrees with the regional present-day direction of maximum stress and is prevalent in the gas-producing top part of the Natih Formation. The secondary fracture set is a production-related feature associated with secondary faults in the field and is prevalent in the Fiqa Shale and the lower parts of the Natih Formation. Finally, a subset of the data that image the middle parts of the Natih shows dominant fast shear-wave polarization of 45°.

The bulk of the anisotropy observed in the Oman field can be attributed to fracture alignment. With more data, spatial variations in the magnitude of the anisotropy potentially could be used to help delineate more heavily fractured regions. That might be important for finding trapped oil and gas in compartmentalized zones. The symmetry of anisotropy and hence orientation of fractures can be used to help guide drilling programs.

Frequency-dependent shear-wave splitting

In many reservoirs, fracture orientation, density, size, and connectivity control reservoir production. Studies of source mechanisms and shear-wave splitting provide insights into fracture orientation and density but offer little information about fracture size and connectivity. Work by Chapman and coworkers (e.g., Maultzsch et al., 2003) has shown that the frequency dependence of shear-wave splitting can be very sensitive to those parameters.

At low seismic frequencies, a material with aligned inclusions will behave like a homogeneous anisotropic medium, but at higher frequencies, the inclusions will behave as discrete scatterers. Poroelastic effects are more subtle. For example, aligned fluid-filled fractures in a porous medium will exhibit frequency-dependent anisotropy. At high frequencies, the inclusions will be isolated and the effective anisotropy will be smaller, whereas at low frequencies, the inclusions effectively are interconnected and the anisotropy will be larger.

Microseismic data are typically rich in frequency content, making them ideal for studies of frequency-dependent wave phenomena, such as Q estimation. The frequency content of the Oman data set is somewhat variable with depth and lithology but is generally between 10 and 400 Hz. The P-waves have higher frequency content than the S-waves.

Al-Anboori et al. (2006b) describe the analysis of frequency-dependent shear-wave splitting in the Oman data set. Data are filtered with a one-octave passband (i.e., a constant ratio of high to low frequencies of 2). Then the splitting parameters are estimated for each frequency band. The results reveal lithology-dependent variability in the nature of frequency-dependent shear-wave splitting.

Figure 8 shows the results for the Fiqa Shale and Natih A carbonate, including a best-fit inversion for fracture size based on the Chapman (2003) model. Results for events confined to the Natih A carbonate formation show a clear and fairly consistent pattern of frequency-dependent shear-wave splitting. Results confined to the Fiqa Shale Formation show no evidence of frequency-dependent shear-wave splitting. The Chapman (2003) model that best fits the results for the Natih A Formation suggest that the anisotropy is caused by cracks or fractures that have an average length of approximately 2 m and high fracture density of 0.07 to 0.23, as might be expected for a reservoir with hydrocarbon production facilitated primarily by fractures.

In contrast, results for the Fiqa suggest that the anisotropy is caused by fine-scale cracks less than 1 mm in size with a moderate fracture density of 0.03 to 0.05, as might be expected for a caprock that is acting as a seal for the reservoir. Al-Anboori et al. (2006a), who explore the robustness of those results by using a grid search over misfit between model parameters (fracture size and density), find that those parameters are constrained well.

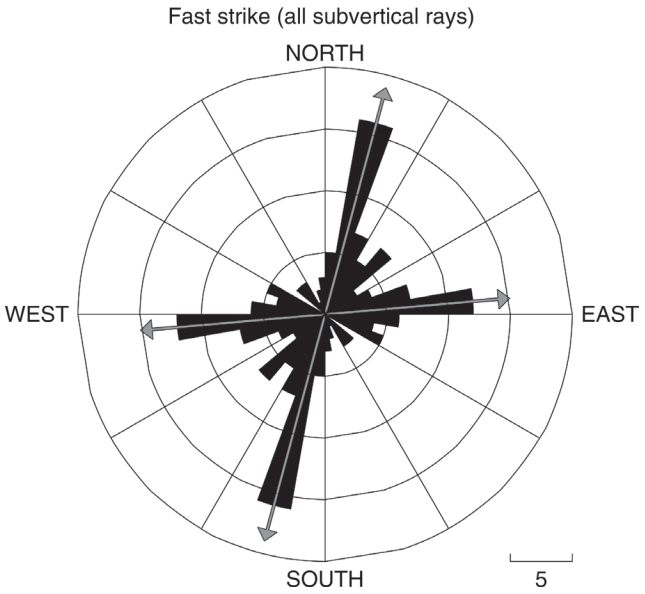

Figure 7. Rose diagram of the strike of fast shear-wave polarization for waves that propagate subvertically. Two average orientations are visible, one at 15° and one at 84°.

Summary and future work

These results show how microseismic data can be used to infer faulting and stress regimes within reservoirs and fracture characteristics such as size, density, and orientation. Figure 9 summarizes the results and demonstrates that fault mechanisms and anisotropy are sensitive to lithology and fractures. Such information is obviously useful in reservoir management. We have analyzed only a limited amount of data from the Oman field. With more data, we can assess not only spatial but also temporal variations in stress-related properties of the field.

As passive seismic monitoring becomes more commonplace, the size and quality of data sets will improve. With ever larger data volumes, there is considerable incentive to automate the analyses. De Meersman et al. (2006) have developed an automated approach for picking traveltimes and particle motions. They show that a semiautomated repicking of P-wave and S-wave arrival times and array-based P-wave polarization analysis improve the accuracy of locations. That also removed some of the subjectivity of manual picking. However, this array-based analysis requires waveform coherency across the recording arrays, which will not be possible if events lie too close to the receivers. It is also possible to automate

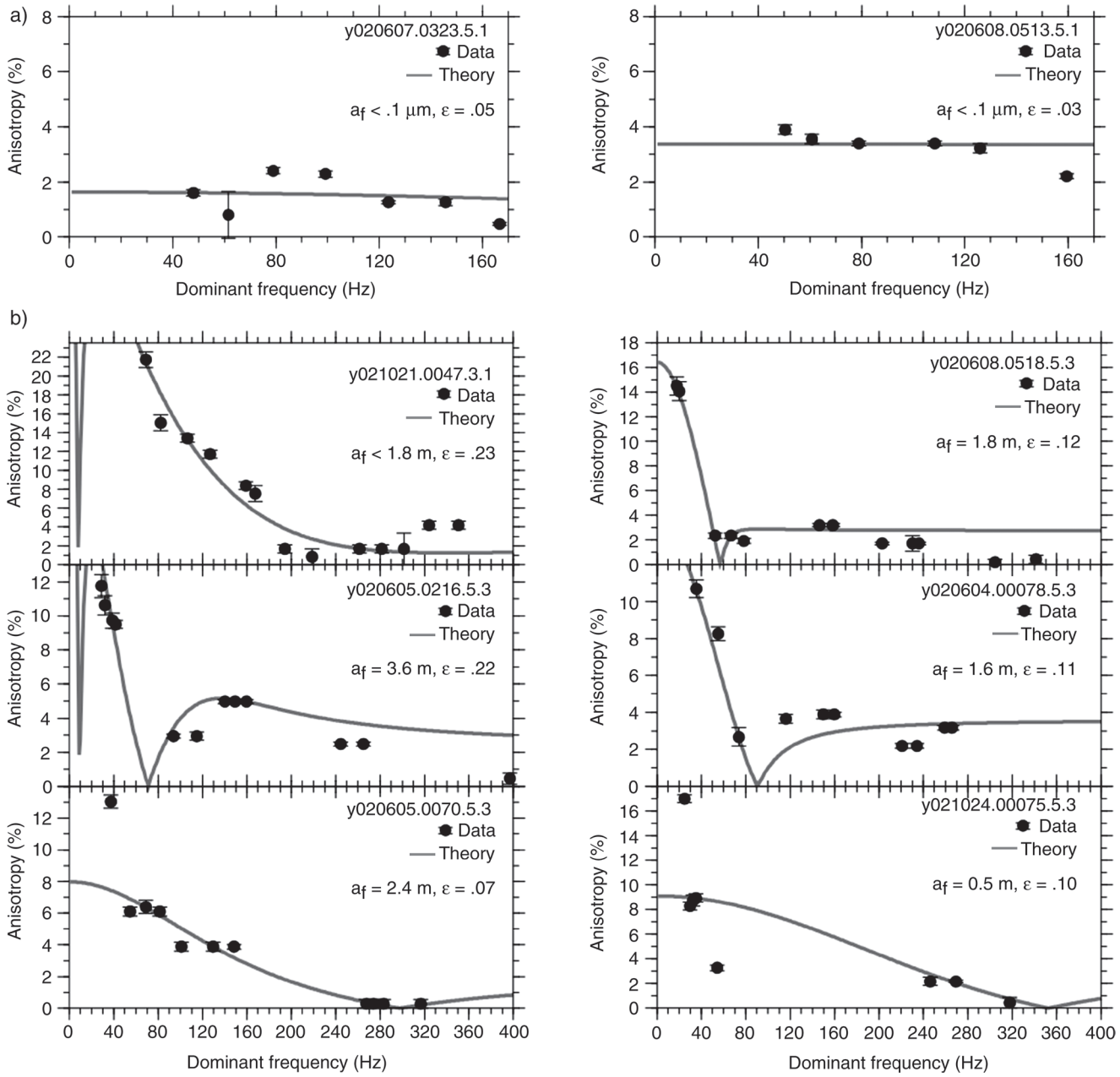

Figure 8. Analysis of frequency-dependent shear-wave splitting in (a) events confined to the Fiqa Formation and (b) events confined to the Natih A Formation. Data measurements are shown with errors as black dots. The splitting magnitude is converted to percentage of anisotropy, assuming anisotropy is distributed evenly along the raypath. Results for the best-fitting crack model based on the poroelastic model of Chapman (2003) are shown as a gray line. The best-fit fracture length and crack density are indicated in the top right of each diagram.

shear-wave splitting analysis, especially once S-wave traveltime picks have been made (Teanby et al., 2004b).

It is much cheaper and logistically simpler to record microseismic events with receivers deployed at the surface. However, microseismic events are generally very weak and therefore difficult to observe with surface sensors. However, it is increasingly common for large surface arrays to be left in place for time-lapse surveys. If such arrays are left to record passively between surveys, stacking methods can be used to accentuate subtle events buried in noise on single traces. That is an inherently 4D problem that is computationally intensive because events must be located in space and time. Nevertheless, recent studies have produced promising results (Duncan, 2005; Chambers et al., 2007).

As a community, we are only starting to scratch the surface of potential uses for passive seismic monitoring as a reservoir-management tool (Maxwell and Urbancic,

2001). The broad range of potential applications of microseismic monitoring can be summarized as follows:

- estimating magnitude and orientation of the stress tensor
- predicting stress buildup and potentially mitigating wellbore failure
- imaging fault and fracture orientations and their reactivation
- characterizing seismic anisotropy, which can be used to determine anisotropy parameters for processing and to assess lithology and fracture-set properties, including orientation, density, and size
- studying fluid properties by using frequency-dependent wave characteristics (e.g., Q estimation and frequency-dependent shear-wave splitting)
- monitoring injection fronts such as water, CO_2, and steam
- monitoring hydraulic fracturing, especially in tight-gas shales and sands
- studying compaction effects around reservoirs
- studying caprock integrity
- studying sealing faults and reservoir compartmentalization
- identifying seismically active and potentially hazardous zones

Microseismicity studies already are used routinely in monitoring fracture propagation caused by hydraulic stimulation. Some key areas for future development include better assessment of the state of stress in tight-gas shales and sands and monitoring long-term CO_2 sequestration in underground reservoirs. Understanding microseismicity is linked intimately to understanding the fluid and geomechanical properties of a reservoir. Future work will see modeling that links reservoir fluid flow, geomechanics, and seismic properties and will use those results to help guide data analyses.

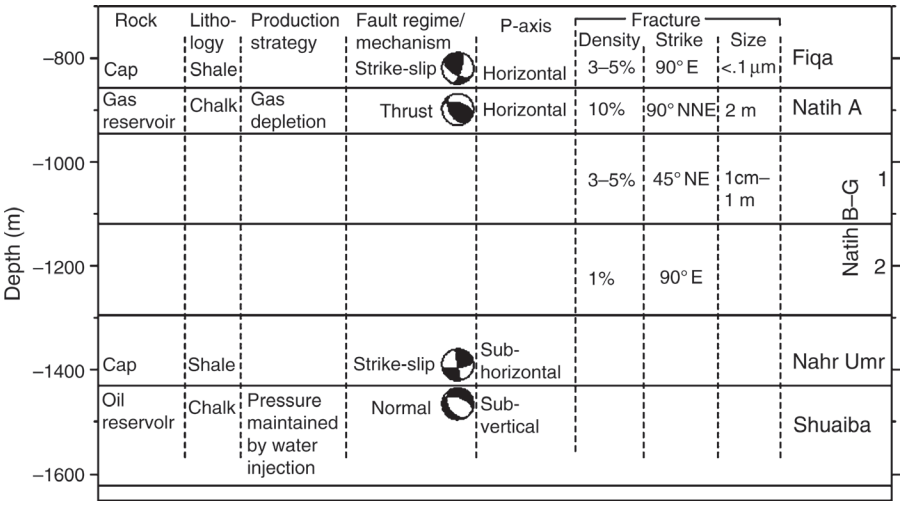

Figure 9. Summary of the key results derived from this study of microseismic activity using analysis of fault-plane solutions and shear-wave splitting. The shale caprocks show mechanisms with strong strike-slip components. The oil-producing Shuaiba shows normal faulting, whereas the upper Natih shows reverse faulting. Anisotropy is strongest in the heavily fractured upper parts of the Natih Formation and weakest in the nonproducing lower parts of the formation. The cause of the anisotropy is attributed to microcracks in the Fiqa Shale and meter-scale fractures in the upper parts of the Natih. Data coverage was insufficient to study anisotropy in the Nahr Umr and Shuaiba.

Acknowledgments

We are grateful to Petroleum Development Oman and the Oman Ministry of Oil and Gas for support and permission to present the microseismic data. We thank Mike Payne, Daniel Raymer, Quentin Fisher, and James Wookey for constructive comments that improved the manuscript.

References

Al-Anboori, A., J-M. Kendall, D. Raymer, and R. Jones, 2005, Microseismic monitoring and spatial variations in anisotropy, an example from Oman: 67th Conference and Exhibition, EAGE, Extended Abstracts, P094.

———, 2006a, Spatial variations in microseismic focal mechanisms, _____ field, Oman: 68th Conference and Exhibition, EAGE, Extended Abstracts, A048.

Al-Anboori, A., J-M. Kendall, and M. Chapman, 2006b, Fracture-induced frequency-dependent anisotropy, _____ field, Oman: 68th Conference and Exhibition, EAGE, Extended Abstracts, A047.

Bourne, S. J., 2006, Monitoring reservoir deformation on land — Evidence for fault reactivation from microseismic, InSAR and GPS data: 68th Conference and Exhibition, EAGE, Extended Abstracts, E026.

Chambers, K., J. M. Kendall, O. Barkved, S. Brandsberg-Dahl, and G. A. Jones, 2007, Imaging micro-seismicity using surface sensors: 69th Conference and Exhibition, EAGE, Extended Abstracts, A039.

Chapman, M., 2003, Frequency-dependent anisotropy due to meso-scale fractures in the presence of equant porosity: Geophysical Prospecting, **51**, no. 5, 369–370.

De Meersman K., M. van der Baan, and J-M. Kendall, 2006, Signal extraction and automated polarisation analysis of multi-component array data: Bulletin of the Seismological Society of America, **96**, no. 6, 2415–2430.

Duncan, P. M., 2005, Is there a future for passive seismic?: First Break, **23**, no. 6, 111–115.

Eisner, L., and J. Sileny, 2004, Moment tensors of events induced in Cotton Valley gas field from waveform inversion: 66th Conference and Exhibition, EAGE, Extended Abstracts, P227.

Gephart, J. W., and D. W. Forsyth, 1984, An improved method for determining the regional stress tensor using earthquake focal mechanism data: Application to the San Fernando earthquake sequence: Journal of Geophysical Research, **89**, B11, 9305–9320.

Jones, R. H., and H. Asanuma, 2004, The tetrahedral geophone configuration: Geometry and properties: 74th Annual International Meeting, SEG, Expanded Abstracts, 9–12.

Kendall, J-M., Q. J. Fisher, S. Covey-Crump, J. Maddock, A. Carter, S. A. Hall, J. Wookey, S. L. A. Valcke, M. Casey, G. Lloyd, and W. Ben Ismail, 2007, Seismic anisotropy as an indicator of reservoir quality in siliciclastic rocks, *in* S. Jolley, D. Barr, J. Walsh, and R. J. Knipe, eds., Structurally complex reservoirs: Geological Society [London] Special Publication 292, 123–136.

Litsey, L. R., W. L. MacBride Jr., K. M. Al-Hinai, and N. B. Dismukes, 1986, Shuaiba reservoir geological study, _____ field, Oman: Journal of Petroleum Technology, **38**, no. 6, 651–661.

Maultzsch, S., M. Chapman, E. Liu, and X.-Y. Li, 2003, Modelling frequency-dependent seismic anisotropy in fluid-saturated rock with aligned fractures: Implication of fracture size estimation from anisotropic measurements: Geophysical Prospecting, **51**, no. 5, 381–392.

Maxwell, S. C., and T. I. Urbancic, 2001, The role of passive microseismic monitoring in the instrumented oil field: The Leading Edge, **20**, no. 6, 636–639.

Mueller, G., H. Rynja, K. Maron, D. Raymer, and R. H. Jones, 2004, Microseismic monitoring of the _____ oilfield: 66th Conference and Exhibition, EAGE, Extended Abstracts, A007.

Rutledge, J. T., W. S. Phillips, and M. J. Mayerhofer, 2004, Faulting induced by forced fluid injection and fluid flow forced by faulting: An interpretation of hydraulic-fracture microseismicity, Carthage Cotton Valley field, Texas: Bulletin of the Seismological Society of America, **94**, no. 5, 1817–1830.

Segall, P., 1989, Earthquakes triggered by fluid extraction: Geology, **17**, no. 10, 942–946.

Snoke, J. A., J. W. Munsay, A. G. Teague, and G. A. Bollinger, 1984, A program for focal mechanism determination by combined use of polarity and SV-P amplitude ratio data: Earthquake Notes, **55**, no. 3, 15.

Teanby, N., J.-M. Kendall, R. H. Jones, and O. I. Barkved, 2004a, Stress-induced temporal variations in seismic anisotropy observed in microseismic data: Geophysical Journal International, **156**, 459–466.

Teanby, N., M. van der Baan, and J.-M. Kendall, 2004b, Automation of shear-wave splitting measurements using cluster analysis: Bulletin of the Seismological Society of America, **94**, no. 2, 453–463.

Wilson, S., R. Jones, W. Wason, D. Raymer, and P. Jaques, 2004, Passive seismic monitoring makes sense for 4D reservoir monitoring: First Break, **22**, no. 10, 59–66.